

Characterization of Self-Similar Multifractals with Wavelet Maxima

*Wen-Liang Hwang and Stephane Mallat*¹ **Technical Report 641**

July 1993

Courant Institute of Mathematical Sciences
Computer Science Department
New York University
251 Mercer Street
New York, NY 10012, USA

Abstract

Self-similar multifractals have a wavelet transform whose maxima define self-similar curves in the scale-space plane. We introduce an algorithm that recovers the affine self-similarity parameters through a voting procedure in the corresponding parameter space. The voting approach is robust with respect to renormalization noises and can recover the value of parameters having random fluctuations. We describe numerical applications to Cantor measures, dyadic multifractals and to the study of Diffusion Limited Aggregates.

¹This research was supported by the AFOSR grant F49620-93-1-0102 and ONR grant N00014-91-J-1967 and the Alfred Sloan foundation

1 Introduction

Some important classes of multifractals are composed of functions which are partly self-similar. The applications of Iterated Functional Systems have shown the importance of such fractals in image processing [6]. Some physical phenomena such as fully developed turbulence [12] or diffusion limited aggregates [1] also seem to exhibit some sort of self-similarity. The synthesis of self-similar fractals is a relatively simple algorithmic issue but the analysis of the affine self-similarities of functions or measures is a more difficult inverse problem. For physical dynamical systems that are believed to have some renormalization properties, it is particularly important to have processing techniques that can estimate the renormalization parameters from the experiments. We introduce a voting algorithm that can recover such renormalization parameters from noisy data.

A multifractal might have different renormalization properties at different scales. The necessity to decouple the multiscale components of signals motivates the use of a wavelet transform to analyze their renormalization parameters. The renormalization properties of a function appears through self-similarities of its wavelet transform, in the scale-space plane. For many types of problems, it is easier to analyze the properties of the wavelet transform local maxima rather than the values of the transform at all locations. In particular, we proved that these local maxima locate and characterize the singularities of functions [11]. The wavelet transform maxima define geometrical curves in the scale-space plane. The self-similarities of a function appear as geometrical self-similarities of the wavelet transform maxima curves. We thus concentrate on these local maxima to analyze the renormalization properties of multifractals.

The multiplicative properties of the wavelet transform maxima is directly related to the parameters of affine self-similar multifractals. This was proved by Bacry et. al. [4] in the case of Cantor measures. For more general class of multifractals, they conjectured that these multiplicative properties is related to the fractal dimension of the singular support. We verify this result for fractional Brownian motions. Most multifractals encountered in physics or image processing are not exactly self-similar. The deviations from self-similarity can be interpreted as a renormalization noise. Voting procedures such as the Hough transform [5], have been particularly successful to recover parameterized curves from noisy data. We introduce such a voting scheme to estimate the renormalization parameters of the wavelet transform maxima curves. Section 4 gives numerical results for a Cantor measure, a dyadique

multifractal function, and a fractional Brownian motion. An application to Diffusion Limited Aggregates is described in Section 5.

2 Self-Similar Multifractals

An interesting class of multifractal functions is solution of dilation functional equations of the type

$$f(x) = \sum_{i=1}^n p_i l_i f(l_i(x - r_i)). \quad (1)$$

The solution might not be a function but a distribution, possibly a positive measure. Throughout the article, functions and measures do not need to be differentiated beyond few details of notations that are left to the reader. If the solution $f(x)$ has a finite non-zero integral, integrating both sides of this equation yields

$$\sum_{i=1}^n p_i = 1.$$

If each affine renormalization operation is locally separable, which means that for $1 \leq i \leq n$ there exists an open set D_i such that for all $x \in D_i$

$$f(x) = p_i l_i f(l_i(x - r_i)), \quad (2)$$

the function is locally self-similar. For number of recurrence equations, $f(x)$ is only approximatively equal to the renormalized version on the right hand-side of equation (2), which introduces what we call a renormalization noise.

Multifractal Cantor measures satisfy a recurrence equation (1) with two separable renormalization components:

$$f(x) = p_1 l_1 f(l_1(x - r_1)) + p_2 l_2 f(l_2(x - r_2)). \quad (3)$$

The renormalization parameters satisfy

$$\begin{aligned} r_1 - \frac{1}{2l_1} &= -\frac{1}{2} \quad , \\ r_1 + \frac{1}{2l_1} &\leq r_2 - \frac{1}{2l_2}, \\ r_2 + \frac{1}{2l_2} &= \frac{1}{2} \quad , \end{aligned}$$

$$p_1 + p_2 = 1, \quad p_1 \geq 0, \quad p_2 \geq 0.$$

A Cantor measure has a support included in the interval $[-\frac{1}{2}, \frac{1}{2}]$. It can be constructed recursively as follows. We define a uniform measure on $[-\frac{1}{2}, \frac{1}{2}]$ and divide it into three pieces: a uniform measure of probability p_1 on the interval $[-\frac{1}{2}, -\frac{1}{2} + \frac{1}{l_1}]$, a zero measure on the interval $[-\frac{1}{2} + \frac{1}{l_1}, \frac{1}{2} - \frac{1}{l_2}]$, and a uniform measure of probability p_2 on the interval $[\frac{1}{2} - \frac{1}{l_2}, \frac{1}{2}]$. The left and right pieces of the resulting measure are then subdivided recursively with the same renormalization operations. The separability property (2) is satisfied for the domains $D_1 =]-\frac{1}{2}, -\frac{1}{2} + \frac{1}{l_1}[$ and $D_2 =]\frac{1}{2} - \frac{1}{l_2}, \frac{1}{2}[$.

The global singular properties of a multifractal is characterized by the spectrum of singularity $f(\alpha)$, which is the Hausdorff dimension of the set of points where the multifractal has singularities of strength α . For a Cantor, the support of $f(\alpha)$ is an interval $[\alpha_1, \alpha_2]$, with $\alpha_1 = -\frac{\log p_1}{\log l_1}$ and $\alpha_2 = -\frac{\log p_2}{\log l_2}$ [9]. If $\alpha = \alpha_1 = \alpha_2$, then all singularities have the same strength and the Cantor is a uniform fractal of dimension α .

If a multifractal is self-similar with respect to affine transformations as in equation (2), then it is also self-similar with respect to any combination of these affine transforms and their inverse. The composition of n affine transforms whose parameters are (p_1, l_1, r_1) with m transforms of parameters (p_2, l_2, r_2) , is an affine transform with parameters $(p_1^n p_2^m, l_1^n l_2^m, r_{n,m})$, where $r_{n,m}$ depends upon l_1, l_2, r_1, r_2 , and the order in which the affine transforms have been applied. If we combine as well the inverse of these transforms, we obtain the same result for $n \in \mathbf{Z}$ and $m \in \mathbf{Z}$. Our goal is to recover the basic affine transforms that renormalize any given multifractal and which yields by recombinations all other affine transforms that renormalize this multifractal.

3 Wavelet Transform Maxima of Multifractals

The wavelet transform is a natural tool to analyze the multifractal properties of signals since it separates their multiscale components. Arneodo, Bacry and Muzy [2] have studied its application to several types of physical multifractals. A wavelet is a function $\psi(x)$ such that

$$\int_{-\infty}^{+\infty} \psi(x) dx = 0. \quad (4)$$

The wavelet transform of a function at the abscissa x and scale s is defined by

$$Wf(s, x) = \int_{-\infty}^{+\infty} f(u) \frac{1}{s} \psi\left(\frac{x-u}{s}\right) du. \quad (5)$$

The wavelet transform of a measure $d\mu$ is defined by replacing $f(u)du$ by $d\mu(u)$. Dilations and translations of functions yield simple modifications of their wavelet transform. Let $g(x) = plf(l(x-r))$, we derive from (5) that

$$Wg(s, x) = plWf(ls, l(x-r)). \quad (6)$$

Let us suppose that our wavelet has compact support included in the interval $[-K, K]$. If a function satisfies the self-similarity property

$$\forall x \in]a, b[, \quad f(x) = plf(l(x-r)), \quad (7)$$

then for any s such that $s < \frac{b-a}{K}$,

$$\forall x \in [a + Ks, b - Ks], \quad Wf(s, x) = plWf(ls, l(x-r)). \quad (8)$$

The self-similarity of $f(x)$ implies a self-similarity of its wavelet transform in the scale-space plane. However the converse is not true. If the wavelet has n vanishing moments, then a self-similarity of the wavelet transform implies a self-similarity of $f(x)$ up to a polynomial of degree n . Indeed, for such wavelets, the wavelet transform ignores polynomial components of degree n . Moreover, the wavelet transform might be self-similar on a limited range of scales, which does not imply a self-similarity of $f(x)$, but still proves the existence of a partial affine self-similarity. Hence, the wavelet transform self-similarities provide a finer description of the signal renormalization properties.

The wavelet transform is a two dimensional function and thus represents a large amount of data to process. To characterize the singular behavior of functions, it is sufficient to process the values and position of the wavelet transform modulus maxima [11]. These modulus maxima have been used by Bacry et al. [4] to compute the spectrum of singularities of multifractals. Let us remind that a wavelet modulus maxima is a point (s_0, x_0) of the scale-space plane, where $|Wf(s_0, x)|$ is locally maximum for x in a neighborhood of x_0 . These maxima are located along curves in the scale-space plane (s, x) . Let $Mf(s, x)$ be the maxima map defined by $Mf(s, x) = Wf(s, x)$ if (s, x) is a modulus maximum, and $Mf(s, x) = 0$ otherwise. Equation (8) implies that

$$\forall x \in [a + Ks, b - Ks], \quad Mf(s, x) = plMf(ls, l(x-r)). \quad (9)$$

The geometry of the maxima curves are thus self-similar in the scale-space plane. Fig. 1(b) shows the wavelet transform of a devil staircase. This function is the primitive of a Cantor measure built with parameters $p_1 = \frac{2}{3}$, $p_2 = \frac{1}{3}$, $l_1 = 2$ and $l_2 = 4$. Fig. 1(c) displays the position of the modulus maxima in the same scale-space plane. The self-similarities of the wavelet transform and of the maxima map corresponds to the self-similarities of the underlined Cantor measure. The wavelet used to compute this transform is shown in Fig. 2(a). The choice of wavelets to detect and characterize singularities is further discussed in [11].

As a consequence of equation (9), we can expect that the number of modulus maxima increases when the scale decreases. Let $f(x)$ be a Cantor measure with dilation scales l_1 and l_2 . Let $N(s)$ be the number of modulus maxima of the wavelet transform. We suppose that $\psi(x)$ is such that the number of maxima is bounded at any scale:

$$\forall s_0 > 0, \exists K_0, \forall s \geq s_0, \quad N(s) \leq K_0. \quad (10)$$

Bacry, Muzy and Arneodo proved that [4] the decay of $N(s)$ satisfies

$$\lim_{s \rightarrow 0} \frac{\log N(s)}{\log s} = \beta, \quad (11)$$

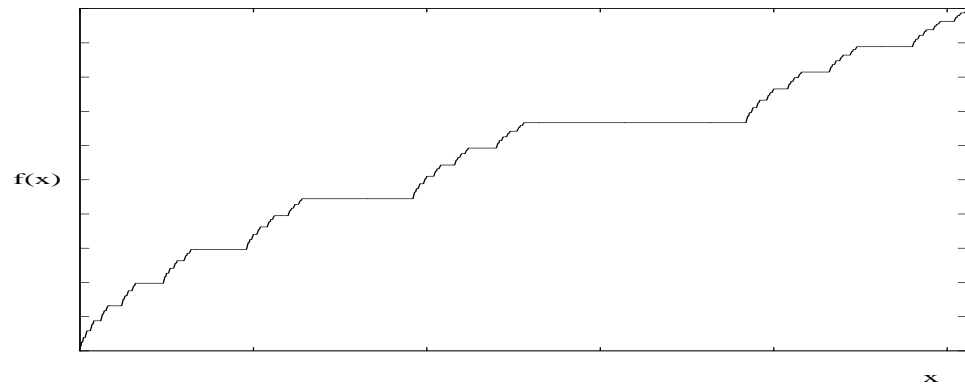
where β is given by

$$l_1^\beta + l_2^\beta = 1. \quad (12)$$

For all wavelets used in practice, the constraint on the finite upper bound (10) is always satisfied. Equation (11) proves that for Cantor measures the decay of the number of maxima depends upon the multiplicative properties of the measure characterized by the dilation scales l_1 and l_2 . When the Cantor measure is uniform, which means that all singularities have a strength equal to $\alpha = -\frac{\log p_1}{\log l_1} = -\frac{\log p_2}{\log l_2}$, since $p_1 + p_2 = 1$, we can derive that $\beta = -\alpha$. For uniform Cantors, the decay rate of the number of maxima is thus equal to their fractal dimension. For general Cantors, $-\beta$ is the fractal dimension of the support of the measure.

Fig. 3 gives the number of maxima across scales corresponding to the wavelet maxima map shown in Fig. 1(c). If we ignore constant factors, the devil staircase has the same renormalization properties as the underlined Cantor measure. A linear regression on the number of maxima in Fig. 1(c) yields $\beta = -0.70$ and indeed

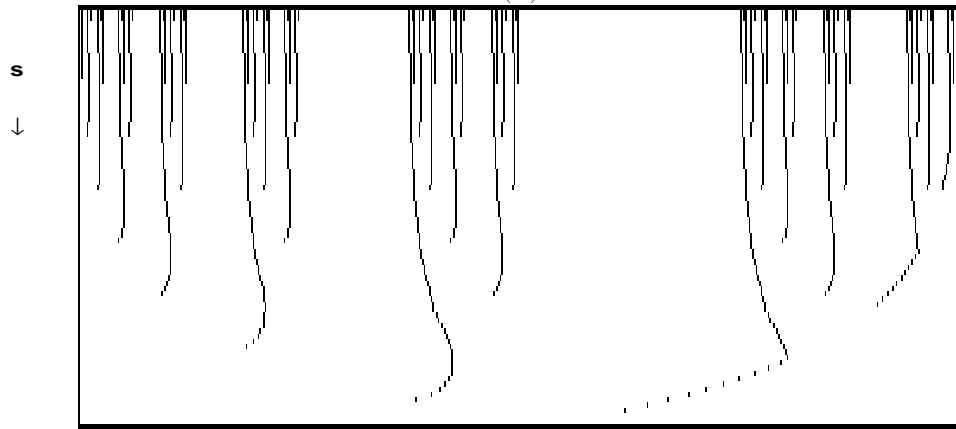
$$2^\beta + 4^\beta = 0.99.$$



(a)



(b)



(c)

Figure 1: (a) Primitive of a Cantor measure constructed with $p_1 = 2/3$, $p_2 = 1/3$, $l_1 = 2$, and $l_3 = 4$. (b) Wavelet transform of the Devil Staircase shown in (a). (c) Modulus maxima of the wavelet transform shown in (b).

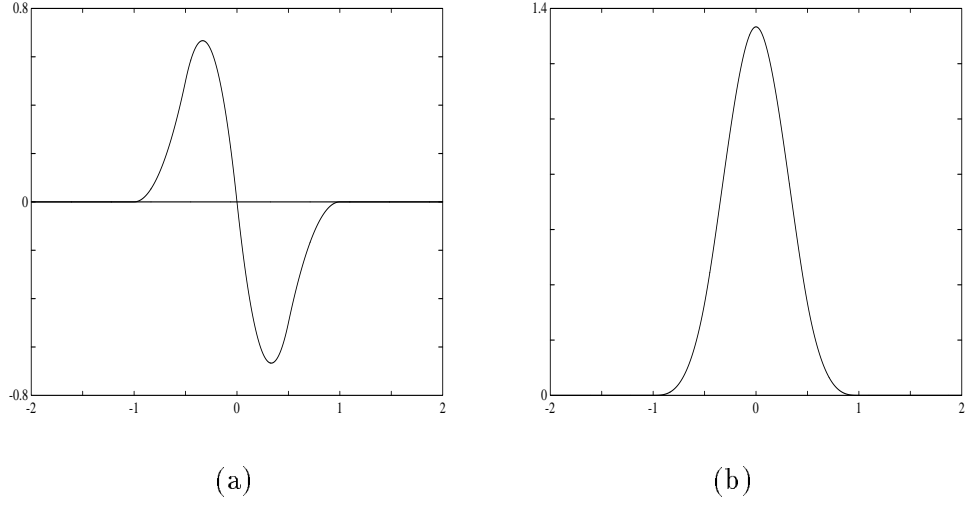


Figure 2: (a) Graph of a wavelet $\psi(x)$ with compact support and one vanishing moment. It is a quadratic spline. (b) Graph of the Primitive $\theta(x)$ with compact support. It is a cubic spline.

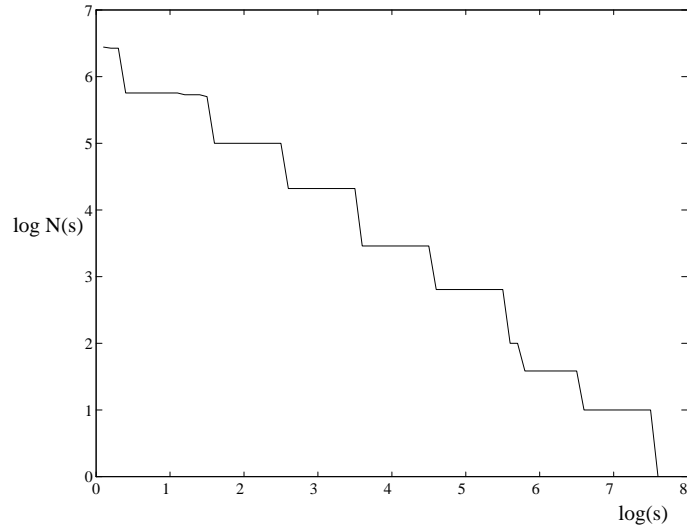


Figure 3: This curve gives the decay of $\log N(s)$ as a function of $\log s$, where $N(s)$ is the number of wavelet transform modulus maxima at the scale s of the Devil Staircase shown in Fig. 1(a).

For more general multifractals, Bacry et. al. [4] conjectured that the number of maxima $N(s)$ decays like s^{-d} where d is the fractal dimension of the singular support of the multifractal. The next theorem verifies this results for fractional Brownian motions. Fractional Brownian motions are Gaussian processes that are self-similar in a stochastic sense, with a power spectrum proportional to $\frac{1}{|\omega|^{2H+1}}$, for some exponent $1 > H > 0$. Their realizations are not affine self-similar functions but fractal curves.

Theorem 1 *The expected density $D(s)$ of modulus maxima of the wavelet transform of a fractional Brownian motion satisfies*

$$D(s) = \frac{C}{s},$$

where C is a constant that depends only upon the wavelet $\psi(x)$ and the fractional exponent H .

The proof of the theorem and the value of the constant C are given in the Appendix. The decay of the number of maxima for fractional Brownian motions is thus inversely proportional to the scale. Since fractional Brownian motions are almost everywhere singular, the fractal dimension of their singular support is $d = 1$, so this theorem verifies the conjecture of Bacry et. al. [4].

4 Vote for Renormalization Parameters

Since the self-similarities of a function implies geometrical self-similarities of the wavelet transform maxima, we concentrate on these maxima to find the values of the renormalization parameters. We can analyze the geometrical properties of the maxima lines in the scale-space plane. This approach was also studied independently by Arneodo, Bacry and Muzy [3], who developed an algorithm based on the bifurcation points of the wavelet transform maxima, in order to detect and characterize renormalization maps. In most cases, multifractals are approximatively self-similar, which means that we must take into account renormalization errors. Many algorithms that estimate the parameters of noisy curves in an image plane are voting procedures in the corresponding parameter space [5]. We describe such a voting algorithm that can recovers non-exact renormalization properties in multifractals by using the information provided by all the wavelet transform maxima.

Affine renormalizations are characterized by the three parameters (p, l, r) of equation (7). We introduce a voting scheme in the three dimensional parameter space (p, l, r) . Renormalization parameters are then identified as points of high votes in the space (p, l, r) . As mentioned in the previous section, if the multifractal is invariant under two affine transformations specified by (p_1, l_1, r_1) and (p_2, l_2, r_2) , it is also invariant with respect to a family of affine transforms specified by $(p_1^n p_2^m, l_1^n l_2^m, r_{n,m})$, where n and m are integers. This produces spurious high vote peaks at the corresponding locations of the parameter space. To obtain a regular distribution of these peaks, we use a logarithmic scale for p and l . In the remaining of the paper, $\log x$ is a logarithm base 2 of x . The parameter space is thus represented by a three dimensional array indexed by $(\log p, \log l, r)$, called accumulator array. Each bin of this array corresponds to a cube in the space $(\log p, \log l, r)$ of size $\Delta \log p \times \Delta \log l \times \Delta r$. The values of $\Delta \log p$, $\Delta \log l$ and Δr depend upon the desired precision when measuring the renormalization parameters.

Equation (6) proves that a renormalization by (p, l, r) maps any wavelet maxima located at (s_1, x_1) to a maxima located at $(s_2 = ls_1, x_2 = l(x_1 - r))$. If $f(x)$ is invariant with respect to the affine transform of parameters (p, l, r) , equation (8) proves that

$$p = \frac{Wf(s_1, x_1)}{l Wf(s_2, x_2)}. \quad (13)$$

Any maxima in the neighborhood of (s_1, x_1) is also mapped to a maxima in the neighborhood of (s_2, x_2) with the same affine transformation. Let $(s_1, x_1 + \Delta_1)$ be the location of the closest maxima to (s_1, x_1) , with $\Delta_1 > 0$. This maxima is mapped to $(s_2, x_2 + \Delta_2)$ with

$$\frac{\Delta_2}{\Delta_1} = \frac{s_2}{s_1}. \quad (14)$$

For any pair of wavelet transform maxima (s_1, x_1) and (s_2, x_2) , if the closest left maxima of (s_1, x_1) and (s_2, x_2) , located respectively at $(s_1, x_1 + \Delta_1)$ and $(s_2, x_2 + \Delta_2)$ satisfy the constraint (14), we then vote for the renormalization parameters

$$\log l = \log\left(\frac{s_2}{s_1}\right), \quad (15)$$

$$\log p = \log\left(\frac{Wf(s_1, x_1)}{l Wf(s_2, x_2)}\right), \quad (16)$$

$$r = x_1 - x_2 \frac{s_1}{s_2}. \quad (17)$$

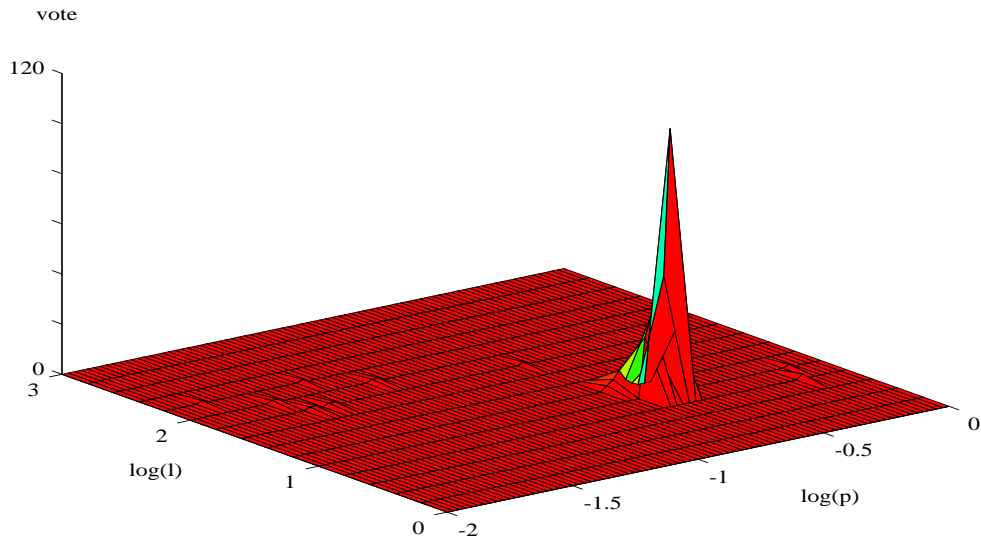
The voting algorithm proceeds as follow. The bins of the parameter space array are first initialized to 0. For each pair of wavelet transform maxima (s_1, x_1) and (s_2, x_2) , with $s_1 < s_2$, if their closest right maxima satisfy equation (14), we add 1 to the bin $(\log p, \log l, r)$ defined by equations (15-17). This algorithm yields high votes in the bins corresponding to the renormalization parameters of the multifractal. The renormalization noise can spread the votes for a given set of renormalization parameters across several bins of the accumulator array. The bin size $\Delta \log p$, $\Delta \log l$, Δr of the accumulator array must therefore be adapted to the amount of renormalization noise in order to avoid splitting votes. Once the vote is done, we select the parameter indexes with high votes, where the value of the vote is locally maximum in a three-dimensional neighborhood of the accumulator array. If the algorithm is successful, the peaks of highest votes provide the renormalization parameters of the multifractal. Instructions to obtain a copy of the software implementing this algorithm are available through anonymous ftp at the address cs.nyu.edu, in the file README of the directory /pub/wave/software.

We first illustrate the results of this algorithm for the devil staircase with $l_1 = 2$, $l_2 = 4$, $p_1 = \frac{2}{3}$, $p_2 = \frac{1}{3}$ and $r_1 = -\frac{1}{4}$, $r_2 = \frac{3}{8}$, shown in Fig. 1(a). The voting is based on the wavelet transform maxima displayed in Fig. 1(c). The highest votes in the three dimensional accumulator array are at $(\log p_1, \log l_1, r_1)$ and $(\log p_2, \log l_2, r_2)$. Since a Cantor set is also invariant by affine transforms of parameters $(p_1^n p_2^m, l_1^n l_2^m, r_{n,m})$ for $(n, m) \in \mathbf{Z}^2$, the algorithm also yields peaks of votes at $(n \log(p_1) + m \log(p_2), n \log(l_1) + m \log(l_2), r_{n,m})$. In the plane $(\log p, \log l)$ these votes are located on a uniform grid whose interval is specified by $(\log p_1, \log l_1)$ and $(\log p_2, \log l_2)$. It allows us to verify that the multifractal only has two sets of renormalization parameters whose values are specified by the locations of the two highest votes in the parameter space. Fig. 4(a) and Fig. 4(b) show the votes in the planes of coordinates $r = -0.26$ and $r = 0.38$, in the three dimensional parameter space $(\log p, \log l, r)$. The two high peaks are the highest votes in the three dimensional parameter space.

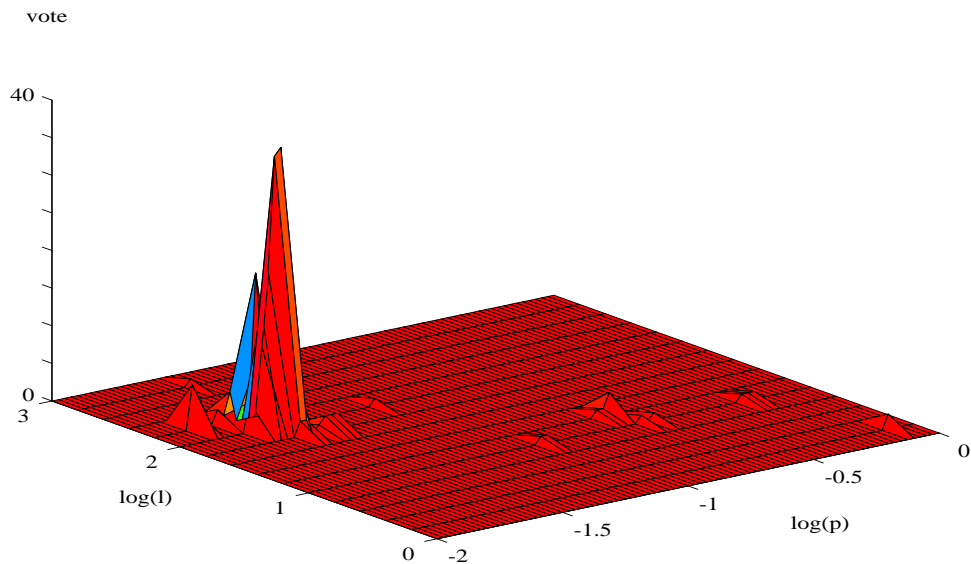
Dyadic renormalization equations also define interesting multifractals studied by Deslauriers and Dubuc [7], as well as Daubechies and Lagarias [10]. The function shown in Fig. 5 is the solution of the functional equation

$$f(x) = \frac{2}{3}f(2(x - \frac{1}{2})) + f(2x) + \frac{1}{3}f(2(x + \frac{1}{2})), \quad (18)$$

analyzed by Daubechies. When applying the voting procedure to the maxima of the wavelet transform of $f(x)$, surprisingly there are 4 peaks that



(a)



(b)

Figure 4: Votes based on the wavelet modulus maxima for the Devil Staircase of Fig. 1(b). These figures give the number of votes in the two planes of the parameter space $(\log p, \log l, r)$, where the highest number of votes are concentrated. The plane (a) corresponds to $r = -0.26$ and the plane (b) to $r = 0.38$. The location of the two high peaks provide the renormalization parameters of the underlined Cantor measure.

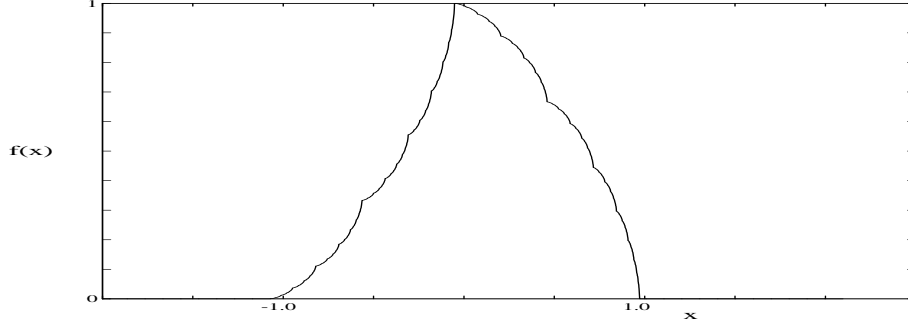
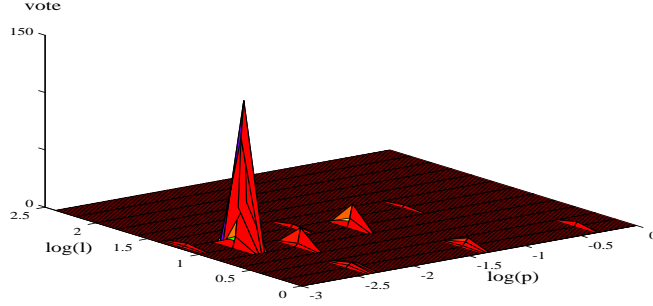


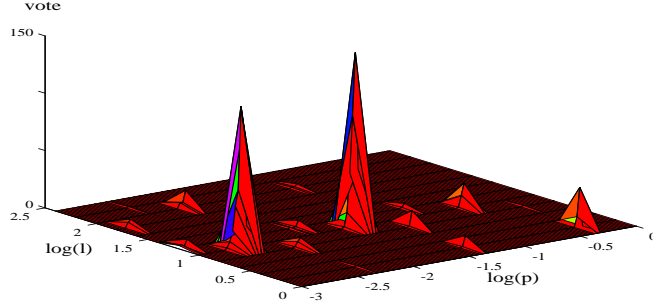
Figure 5: Solution of the functional equation $f(x) = 1/3f(2(x - 1/2)) + f(2x) + 2/3f(2(x + 1/2))$.

emerge strongly from the accumulator array, for parameters (p, l, r) respectively equal to $(\frac{1}{3}, 2, 0)$, $(\frac{1}{6}, 2, 0)$, $(\frac{1}{3}, 2, \frac{1}{2})$ and $(\frac{1}{6}, 2, -\frac{1}{2})$. Fig. 6(a-c) show the votes in the planes corresponding respectively to $r = -\frac{1}{2}$, $r = 0$ and $r = \frac{1}{2}$. Beyond the four peaks, we can see other local peaks of smaller amplitude that correspond to recombinations of the four main affine renormalizations. It is surprising to see four different affine self-similarities since the recurrence equation (18) has only three terms and the parameters can not be derived directly from the coefficients of the equation. However, a more careful analysis of the solution $f(x)$ reveals that these affine transforms are indeed the true renormalization parameters. Let us decompose $f(x)$ into $f(x) = g(x) + h(x)$, where the support of $h(x)$ and $g(x)$ are respectively $[-1, 0]$ and $[0, 1]$. One can prove that $h(x)$ is the primitive of a positive Cantor measure centered at $-\frac{1}{2}$ with parameters $l_1 = 2$, $l_2 = 2$, $p_1 = 1/3$ and $p_2 = 2/3$, and $g(x)$ is the primitive of a negative Cantor measure centered at $\frac{1}{2}$ with parameters $l_1 = 2$, $l_2 = 2$, $p_1 = 1/3$ and $p_2 = 2/3$. In this case, the voting algorithm did indeed reveal non-trivial self-similar structures of the function $f(x)$.

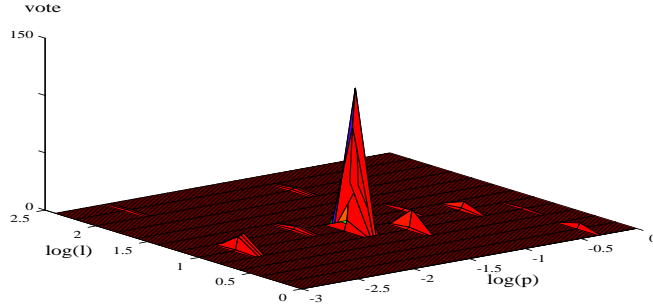
As a last example, we describe the results of this voting algorithm, when applied to a fractional Brownian motion. The realizations of these stochastic multifractals do not have affine self-similarities, and indeed do not yield any dominating peak in the parameter space. To visualize better the distribution of votes in the parameter space, for any given r we sum the votes for all values of p and l . The resulting number of votes as a function of r is given in Fig. 7(a). As expected, this distribution is uniform, which indicates that



(a)

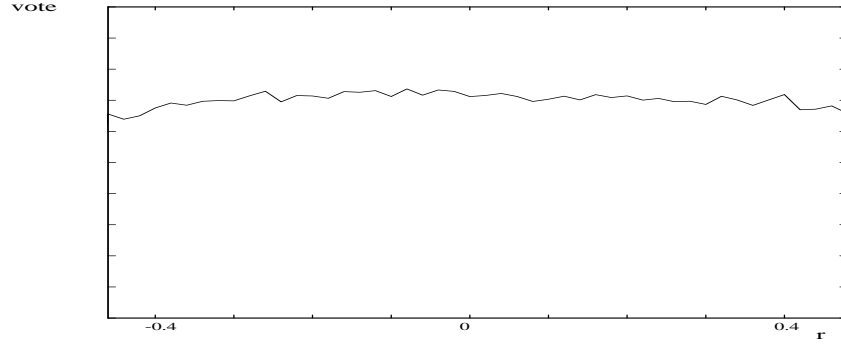


(b)

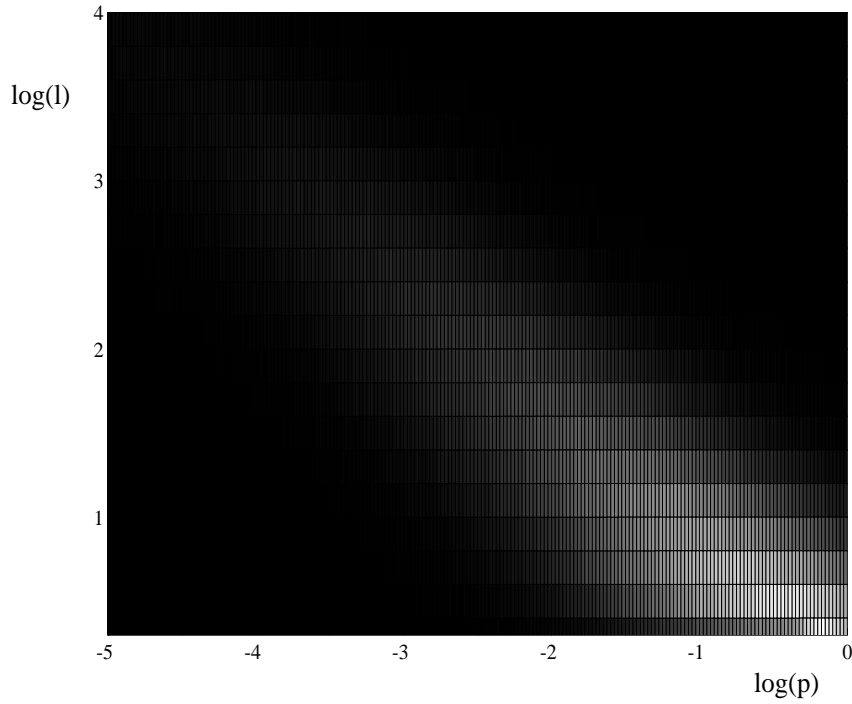


(c)

Figure 6: Votes based on the wavelet transform modulus maxima of the dyadique multifractal shown in Fig. 5. These figures give the number of votes in the three planes of the parameter space $(\log p, \log l, r)$, where the highest number of votes are concentrated. The planes (a),(b) and (c) correspond respectively to $r = -\frac{1}{2}$, $r = 0$ and $r = \frac{1}{2}$. The location of the four high peaks provide the renormalization parameters of this multifractal.



(a)



(b)

Figure 7: Distribution of votes for a fractional Brownian motion with $H = 0.2$. (a) Repartition of votes as a function of r , after summing over all values of $\log l$ and $\log p$. (b) Repartition of the votes in the plane $(\log p, \log l)$, after summing over all values of r . Brighter pixels correspond to larger votes. There is no high peak in (a) and (b).

there is no remarkable translation parameter. For any given $(\log p, \log l)$, we also sum the votes for all r values in the accumulator array and obtain a distribution in the $(\log p, \log l)$ plane, shown in Fig. 7(b). Higher votes correspond to brighter points in the image plane. No particular peak emerges from this plane, but the vote has a clear distribution around a straight line whose equation is $\log p = \beta \log l$, with $\beta = -1.2$. The slope β is related to the fractal parameter $H = 0.2$ of this fractional Brownian motion, by $\beta = -1 - H$. This can be justified with the following intuitive argument. The algorithm votes for a parameters p in equation (13) which is equal to the ratio of the wavelet transform at two maxima locations, divided by l . Flandrin [8] proved that at any point (s_1, x_1) , the variance of the wavelet transform of a fractional Brownian motion satisfies

$$E(|WB(s_1, x_1)|^2) = C s_1^{2H},$$

where C is a constant independent of (x_1, s_1) . Hence the ratio of the wavelet transform at two maxima locations at the scales s_1 and s_2 is on average close to $(\frac{s_1}{s_2})^H = l^{-H}$. The value of $\log p$ will thus on average be of the order of $(-H - 1) \log l$. This explains the higher density of votes around the line of equation $\log p = (-1 - H) \log l$. In this example, the voting algorithm indicates that this fractal has no affine renormalization but we can still measure the fractional exponent H from the repartition of the votes in the $(\log p, \log l)$ plane.

5 Diffusion Limited Aggregates

The analysis of the properties of fractal growth phenomena remains mostly an open problem in physics. Diffusion Limited Aggregates can be modeled as a growth obtained by successive accretion of random walker at the periphery of the cluster. Arneodo et. al. [1] have recently introduced techniques based on the wavelet transform modulus maxima to analyze the fractal properties of these DLA. Fig. 8(a) shows the center region of a DLA cluster that contains a total of 10^8 particles. To analyze the properties of such clusters, Arneodo et. al. [1] have constructed a measure that indicates the location of intersection points of such a cluster with a circle of fixed radius. At intersection points, the measure is equal to 1 and 0 at other locations. Fig. 8(b) such a measure built at the intersection of a circle and a DLA cluster.

The wavelet transform is normally defined with respect to a wavelet function whose integral is zero. However, to analyze positive measures of

compact support, one can use a wavelet primitive whose integral is non-zero, and obtain the same properties as a standard wavelet transform. Let $\psi^1(x)$ be the primitive of compact support of a wavelet $\psi(x)$ of compact support. The function $\psi^1(x)$ might have a non-zero integral and thus might not be a wavelet. Let $f(x)$ be a positive measure of compact support and $g(x)$ be its primitive of compact support. Let us denote $W^1 f(s, x)$ the “pseudo” wavelet transform of $f(x)$ computed with $\psi^1(x)$ by using the same formula (5) as a wavelet transform. Let $Wg(s, x)$ be the wavelet transform of $g(x)$ computed with the wavelet $\psi(x)$. An integration by part of equation (5) yields

$$W^1 f(s, x) = \frac{1}{s} Wg(s, x).$$

Hence, the pseudo wavelet transform of $f(x)$ computed with $\psi^1(x)$ has the same properties as the wavelet transform of its primitive computed with respect to $\psi(x)$. To analyze the properties of DLA measures, we use the wavelet primitive $\psi^1(x)$ shown in Fig. 2(b). Arneodo et. al. [1] showed that the number of maxima of DLA measures at scales 2.2^n is a Fibonacci sequence. One interpretation is that each branch of the DLA splits into two branches, one larger than the other, which then splits recursively with the same procedure. It is however not clear how to relate precisely results on one-dimensional DLA measures to the properties of two-dimensional aggregates. In this section, we analyze the properties of DLA measures from the results of the voting algorithm described in section 4. The experiments are done on 50 DLA measures provided by Arneodo. Fig. 9 gives the number of wavelet modulus maxima $N(s)$, computed with 50 DLA measures, for $s \in [2^2, 2^8]$. A linear regression yields

$$\frac{\log N(s)}{\log s} = -0.63 \pm 0.01. \quad (19)$$

To relate this result to Fibonacci sequences, let us recall that a Fibonacci sequence $(u_n)_{n \in \mathbf{N}}$ satisfies

$$\lim_{n \rightarrow +\infty} \frac{\log(u_n)}{n} = \log(\phi), \quad (20)$$

where $\phi = \frac{1+\sqrt{5}}{2}$. Equation (19) and (20) implies that the number of maxima $N(s)$ may be a Fibonacci sequence along the scales $s = a^n$, if $\alpha = \frac{\log \phi}{\log a}$, which yields $a = 2.13$. This result is consistent with the fact that Arneodo et. al. found that the number of maxima at scales 2.2^n vary almost like Fibonacci sequences.

Let us now study the renormalization properties of these DLA with the voting algorithm. To simplify the analysis we shall concentrate on the parameters p and l and eliminate the translation parameter r . We make a vote for the parameters $(\log p, \log l)$ from the wavelet transform maxima computed with the 50 DLA measures. Fig. 10(a) shows the distribution of the highest votes in the plane $(\log p, \log l)$. The votes are distributed along a line of equation $\log p = -\alpha \log l$, with

$$\alpha = 0.63 \pm 0.01.$$

This indicates that the singularities of strength $\alpha = 0.63$ strongly dominate all other singularities. It is interesting to observe that this exponent is the same as the one measured in equation (19) from the decay of the number of maxima. We saw in section 3 that such a situation occurs for uniform Cantor measures. For example, a uniform Cantor with parameters $l_1 = 2.13$, $l_2 = (2.13)^2$, $p_1 = 0.618$ and $p_2 = 0.382$ does satisfy this property and the number of maxima at the scales a^n for $a = l_1 = 2.13$ is a Fibonacci sequence. This Fibonacci Cantor is built by recursively dividing a uniform measure into two uniform measures. One has a support l_1 times smaller and the other one a support $l_2 = l_1^2$ times smaller. When the branches of a DLA splits, Arneodo observed that the larger branch has one chance out of 2 to be on the right or on the left of the smaller branch. To take into account this fact, one can build a simple stochastic Fibonacci Cantor model where the sub-component of size l_1 is located randomly on the left or on the right of the component of size l_2 , when recursively building the measure. Fig. 10(b) displays in the $(\log p, \log l)$ plane the distribution of votes computed from the wavelet transform maxima of several realizations of this stochastic Fibonacci Cantor. As expected, the votes are distributed around a line of equation $\log p = -\alpha \log l$, with $\alpha = 0.63$.

For any fixed $\log l$, Fig. 11(a) and 11(b) show the distributions of votes as a function of $\log l$ when summing the votes along all $\log p$ for DLA measures and for stochastic Fibonacci Cantors. The vote distribution of stochastic Fibonacci Cantor has three clear peaks at $\log l = 1.1$, $\log l = 2.2$ and $\log l = 3.3$ which are multiples of the basic renormalization parameters $\log l_1 = 1.1$ and $\log l_2 = 2.2$. For the DLA measures, there are two peaks at $\log l = 1.0$ and $\log l = 2.1$ which are much weaker and a third rebound at $\log l = 3.3$, which indicates that this simple stochastic Fibonacci Cantor model do not reflect precisely all structures of the DLA. One can refine the Cantor model by letting the left and right components of the measure have positions that vary randomly when building it recursively, but it is also likely that the multi-

plication process involved in DLA has a more complicated structure than a Cantor subdivision. A more precise analysis of the distribution of the votes of DLA measures that includes the translation component r , can help specify this initial Fibonacci model, but a detailed analysis of the physics of DLA is beyond the scope of this paper. Let us however emphasize that although DLA do not have exact affine self-similarity properties, our maxima voting algorithm recovers enough statistical information about the renormalization parameters, to test physical models of these aggregates. We believe that such robust voting schemes can be used to test a large class of renormalization models for physical multifractals.

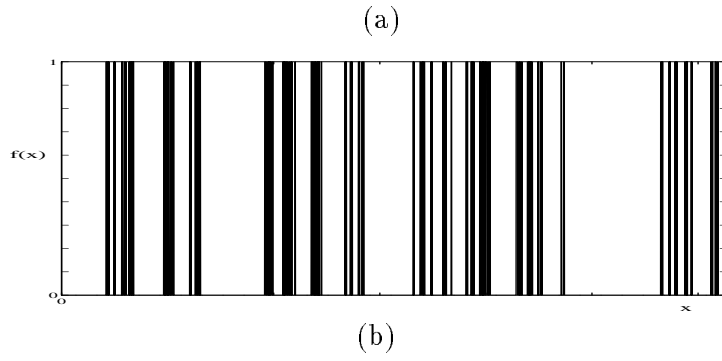


Figure 8: (a) Center region of a DLA cluster of 10^8 particles, which is included in a circle of fixed radius. (b) measure showing the intersection points of a DLA cluster and a circle of fixed radius (data provided by Arneodo).

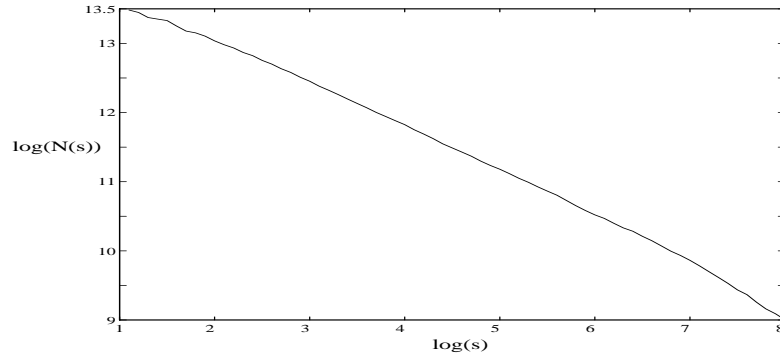
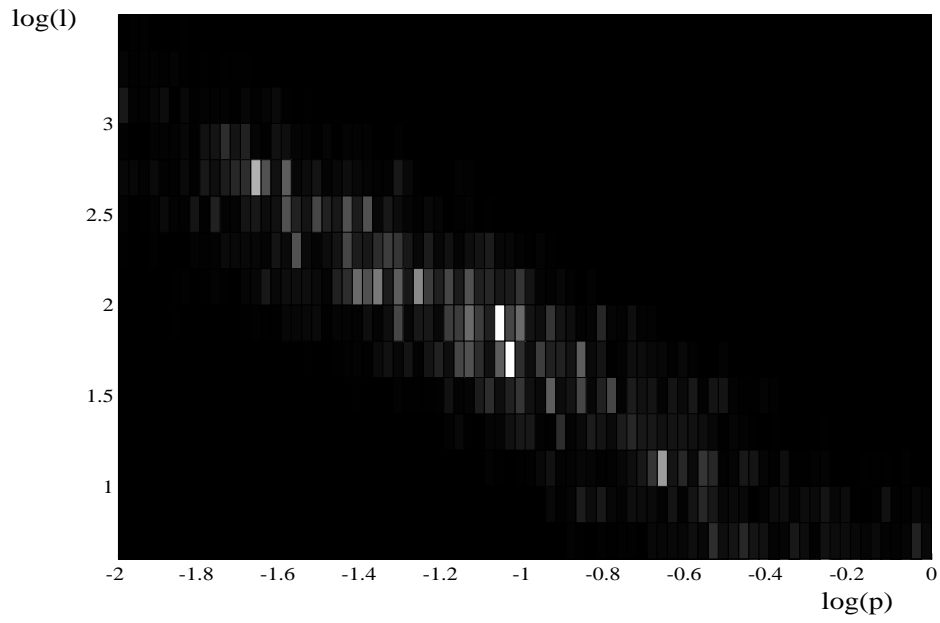
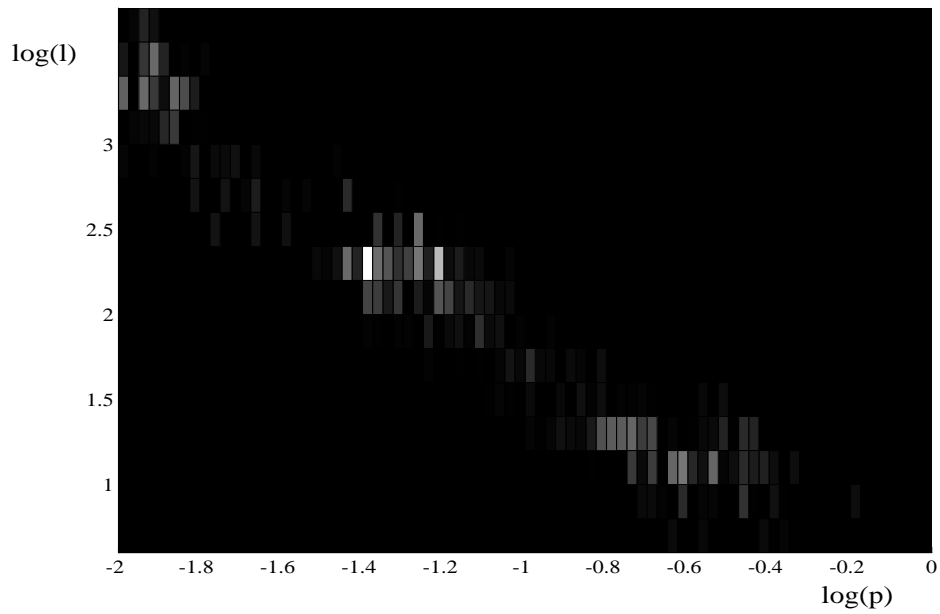


Figure 9: This curve gives the decay of $\log N(s)$ as a function of $\log s$, where $N(s)$ is the number of wavelet transform modulus maxima at the scale s for 50 DLA measures.

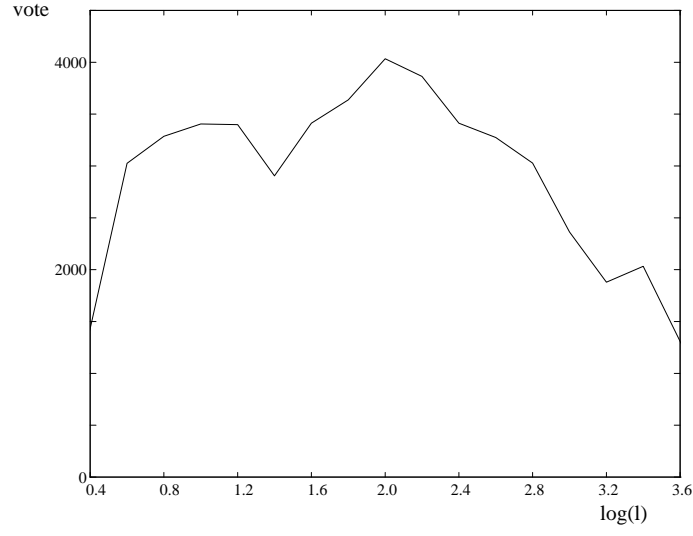


(a)

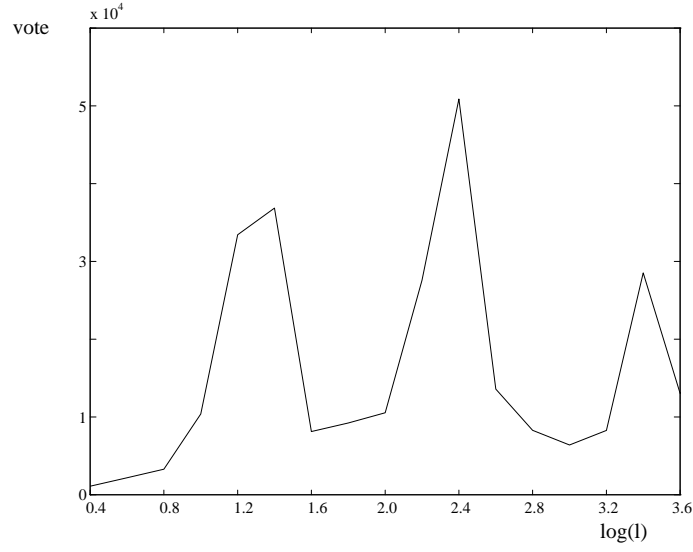


(b)

Figure 10: (a) Distribution of votes in the plane $(\log p, \log l)$ of the parameter space, for 50 DLA measures. The votes are distributed along a straight line of equation $\log p = 0.63 \log l$. (b) Distribution computed for 50 stochastic Fibonacci Cantors.



(a)



(b)

Figure 11: Distribution of votes as a function of $\log l$ obtained from Fig. 10 by summing along all values of $\log p$. (a) Result obtained for 50 DLA measures. (b) Result obtained for 50 stochastic Fibonacci Cantors.

Appendix: proof of Theorem 1

The wavelet transform given in equation (5) can be rewritten a convolution product

$$Wf(s, x) = f \star \psi_s(x), \quad (21)$$

where $\psi_s(x) = \frac{1}{s}\psi(\frac{x}{s})$. The wavelet transform of a fractional Brownian motion is a stationary Gaussian process [8] with a power spectrum $P(\omega)$ equal to

$$P(\omega) = \frac{\sigma^2 |\hat{\psi}(s\omega)|^2}{|\omega|^{2H+1}}, \quad (22)$$

where $\hat{\psi}(\omega)$ is the Fourier transform of $\psi(x)$. The density of m of modulus maxima of a function is related to the density e of local extrema and its density z of zero-crossings by

$$m = \frac{e + z}{2}. \quad (23)$$

The density of zero-crossings of a differentiable Gaussian process whose autocorrelation is $R(\tau)$ is [13]

$$z = \sqrt{\frac{-R^{(2)}(0)}{\pi^2 R(0)}}, \quad (24)$$

where $R^{(n)}(\tau)$ is the n^{th} derivative of $R(\tau)$. The density of extrema of a differentiable process is equal to the density of zero-crossings of the derivative of the process. If the autocorrelation of a process is $R(\tau)$, the autocorrelation of its derivative is $-R^{(2)}(\tau)$. We thus derive from equation (24) that for a stationary Gaussian process that is twice continuously differentiable, the density of extrema is

$$e = \sqrt{\frac{R^{(4)}(0)}{-\pi^2 R^{(2)}(0)}}. \quad (25)$$

The derivatives of the autocorrelation function in zero is related to the power spectrum by

$$R(0) = \int_{-\infty}^{+\infty} P(\omega) d\omega, \quad (26)$$

$$-R^{(2)}(0) = \int_{-\infty}^{+\infty} \omega^2 P(\omega) d\omega, \quad (27)$$

and

$$R^{(4)}(0) = \int_{-\infty}^{+\infty} \omega^4 P(\omega) d\omega. \quad (28)$$

If the wavelet is twice continuously differentiable, the convolution of a Fractional Brownian motion with a dilated wavelet is a stationary Gaussian process that is twice differentiable. Inserting equation (22) in equations (26-28) yields

$$R(0) = \sigma^2 s^{2H} \int_{-\infty}^{+\infty} |\omega|^{-1-2H} |\hat{\psi}(\omega)|^2 d\omega, \quad (29)$$

$$- R^{(2)}(0) = \sigma^2 s^{2H-2} \int_{-\infty}^{+\infty} |\omega|^{1-2H} |\hat{\psi}(\omega)|^2 d\omega, \quad (30)$$

$$R^{(4)}(0) = \sigma^2 s^{2H-4} \int_{-\infty}^{+\infty} |\omega|^{3-2H} |\hat{\psi}(\omega)|^2 d\omega. \quad (31)$$

As a consequence of equation (23), the average density of modulus maxima of a wavelet transform is given by the average density of its zero-crossings and of its extrema. From equations (24-25) and (29-31), we derive that the average density of modulus maxima of the wavelet transform at the scale s of a fractional Brownian motion is

$$D(s) = \frac{1}{s2\pi} \left(\frac{\sqrt{P_4}}{\sqrt{P_2}} + \frac{\sqrt{P_2}}{\sqrt{P_0}} \right), \quad (32)$$

with

$$P_0 = \int_{-\infty}^{+\infty} |\omega|^{-1-2H} |\hat{\psi}(\omega)|^2 d\omega, \quad (33)$$

$$P_2 = \int_{-\infty}^{+\infty} |\omega|^{1-2H} |\hat{\psi}(\omega)|^2 d\omega, \quad (34)$$

and

$$P_4 = \int_{-\infty}^{+\infty} |\omega|^{3-2H} |\hat{\psi}(\omega)|^2 d\omega. \quad (35)$$

This finishes the proof of Theorem 1.

References

- [1] Arneodo, F. Argoul, E. Bacry, J. Muzy and M. Tabard, “Golden mean arithmetic in the fractal branching of diffusion-limited aggregates”, Technical report, Paul-Pascal research center, France, 1991.
- [2] A. Arneodo, E. Bacry and J. Muzy, “Wavelet analysis of fractal signals”, Technical report, Paul-Pascal research center, France, 1991.
- [3] A. Arneodo, E. Bacry and J. Muzy, “Solving the inverse fractal problem from wavelet analysis”, Submit. to Phys Rev. Lett.
- [4] E. Bacry, J. Muzy and A. Arneodo, “Singularity spectrum of fractal signals from wavelet analysis: exact results”, *Journ. of Statistical Physics*, vol. 70, no. 314, 1993.
- [5] D. Ballard, “Generalizing the Hough transform to detect arbitrary shapes”, *Pattern Recognition*, vol. 13, no. 2, p. 111-122, 1981.
- [6] M. Barnsley and A. Sloan, “A better way to compress images”, *Byte Magazine*, January 1988, p. 215-223.
- [7] G. Deslauriers, and S. Dubuc, “Interpolation dyadique”, *Fractals, dimensions non entières et applications*, G. Cherbit, Masson, Paris, 1987.
- [8] P. Flandrin, “Wavelet analysis and synthesis of fractional Brownian motion”, *IEEE Trans. on Information Theory*, vol. 38, no. 2, March 1992.
- [9] T. Halsey, M. Jensen, L. Kadanoff, I. Procaccia and B. Shraiman, “Fractal measures and their singularities: the characterization of strange sets”, *Physical Review A*, vol. 33, no. 2, p. 1141-1151, 1986.
- [10] I. Daubechies, and J. Lagarias, “Two-scale difference equations. Existence and global regularity of solutions”, *SIAM Journ. of Math. Anal.* vol. 22, no. 5, pp. 1388-1410, Sept. 1991.
- [11] S. Mallat and W.L. Hwang, “Singularity detection and processing with wavelets” *IEEE Trans. on Information Theory*, vol. 38, no. 2, March 1992.
- [12] C. Meneveau and K. Sreenivasan, *Phys. Rev., Lett.*, Vol. 59, p. 1424, 1987.

- [13] A. Papoulis “Probability, random variables, and stochastic processes”,
Mc Graw-Hill Book, 1984.